Redesign of Cytochrome *c* Peroxidase into a Manganese Peroxidase: Role of Tryptophans in Peroxidase Activity†

Alan Gengenbach, Sung Syn, Xiaotang Wang, and Yi Lu*

Department of Chemistry, University of Illinois at Urbana-Champaign, Urbana, Illinois 61801

Received March 23, 1999; Revised Manuscript Received June 4, 1999

ABSTRACT: Trp191Phe and Trp51Phe mutations have been introduced into an engineered cytochrome *c* peroxidase (C*c*P) containing a Mn(II)-binding site reported previously (MnC*c*P; see Yeung, B. K.-S., et al. (1997) *Chem. Biol. 5*, 215−221). The goal of the present study is to elucidate the role of tryptophans in peroxidase activity since C*c*P contains both Trp51 and Trp191 while manganese peroxidase (MnP) contains phenylalanine residues at the corresponding positions. The presence of Trp191 in C*c*P allows formation of a unique high-valent intermediate containing a ferryl oxo and tryptophan radical called compound I′. The absence of a tryptophan residue at this position in MnP is the main reason for the formation of an intermediate called compound I which contains a ferryl oxo and porphyrin π-cation radical. In this study, we showed that introduction of the Trp191Phe mutation to MnC*c*P did not improve MnP activity (specific activity: MnC*c*P, 0.750 μmol min^{-1} mg^{-1}; MnC*c*P(W191F), 0.560 μmol min^{-1} mg^{-1}. k_{cat}/K_m: MnC*c*P, 0.0517 s^{-1} mM^{-1}; MnC*c*P(W191F), 0.0568 s^{-1} mM^{-1}) despite the fact that introduction of the same mutation to WTC*c*P caused the formation of a transient compound I (decay rate, 60 s^{-1}). However, introducing both the Trp191Phe and Trp51Phe mutations not only resulted in a longer lived compound I in WTC*c*P (decay rate, 18 s^{-1}), but also significantly improved MnP activity in MnC*c*P (MnC*c*P(W51F, W191F): specific activity, 8.0 μmol min^{-1} mg^{-1}; k_{cat}/K_m, 0.599 s^{-1} mM^{-1}). The increase in activity can be attributed to the Trp51Phe mutation since MnC*c*P(W51F) showed significantly increased MnP activity relative to MnC*c*P (specific activity, 3.2 μmol min^{-1} mg^{-1}; k_{cat}/K_m, 0.325 s^{-1} mM^{-1}). As with MnP, the activity of MnC*c*P(W51F, W191F) was found to increase with decreasing pH. Our results demonstrate that, while the Trp191Phe and Trp51Phe mutations both play important roles in stabilizing compound I, only the Trp51Phe mutation contributes significantly to increasing the MnP activity because this mutation increases the reactivity of compound II, whose oxidation of Mn(II) is the rate-determining step in the reaction mechanism.

Cytochrome *c* peroxidase (C*c*P)[1] from *Saccharomyces cerevisiae* and manganese peroxidase (MnP) from *Phanerochaete chrysosporium* are members of the plant, fungal, and bacterial peroxidase superfamily (*1*−*4*). X-ray crystallographic studies on C*c*P (*5*−*7*) and MnP (*8*) have shown that, despite poor sequence homology, both enzymes (like other members of the superfamily) share close overall structural homology and contain similar heme active sites including the conserved proximal and distal histidines and their hydrogen-bonding partners (Asp on the proximal side and Arg and Asn on the distal side). Both C*c*P and MnP utilize hydrogen peroxide as the terminal oxidant, and yet they perform dramatically different functions. C*c*P is unique among the heme peroxidases in that its biological function is to catalyze the oxidation of another macromolecule, cytochrome *c* (*9*). MnP is involved in the biodegradation of lignin, the second most abundant biopolymer on earth, and many aromatic pollutants including polychlorinated biphenyls (*10*−*12*). Therefore, key structural differences must exist between the two enzymes that are responsible for the functional differences.

Comparison of the X-ray structures for C*c*P and MnP reveals two major differences (Figure 1). First, C*c*P lacks the Mn(II)-binding site that is present in MnP. Second, the number of potentially redox-active amino acid residues differs greatly between the two proteins as C*c*P contains 7 tryptophan and 14 tyrosine residues, whereas MnP has only one tryptophan and no tyrosine residues. Extensive biochemical and spectroscopic studies show these structural differences are manifested as differences in the catalytic mechanism of the two enzymes (Figure 2) (*10*−*12*). While C*c*P directly oxidizes cytochrome *c*, the manganese-binding

† This work is supported by the National Science Foundation under Award CHE 95-02421 to Y.L. (CAREER Award and Special Creativity Extension). Y.L. is a Sloan Research Fellow of Alfred Sloan Foundation, a Cottrell Scholar of the Research Corp., a Camille Dreyfus Teacher−Scholar of the Camille and Henry Dreyfus Foundation, and a Beckman Young Investigator of the Arnold and Mabel Beckman Foundation.

* To whom correspondence should be addressed. Tel: (217) 333-2619. Fax: (217) 333-2685. E-mail: yi-lu@uiuc.edu.

[1] Abbreviations: C*c*P, cytochrome *c* peroxidase from *Saccharomyces cerevisiae*; MnP, manganese peroxidase; APX, ascorbate peroxidase; WTC*c*P, wild-type yeast C*c*P; C*c*P(MI), recombinant yeast C*c*P containing Met-Ile at the N-terminus in addition to the normal WTC*c*P sequence; MnC*c*P, C*c*P(MI, G41E, V45E, H181D); MnC*c*P(W191F), C*c*P(MI, G41E, V45E, H181D, W191F); MnC*c*P(W51F), C*c*P(MI, G41E, V45E, W51F, H181D); MnC*c*P(W51F, W191F), C*c*P(MI, G41E, V45E, W51F, H181D, W191F); ferryl, heme Fe(IV)═O; compound I, ferryl and porphyrin π cation radical; compound I′, ferryl and Trp radical; UV−vis, electronic absorption in the ultraviolet and visible regions.

10.1021/bi990666+ CCC: $18.00
Published on Web 08/07/1999

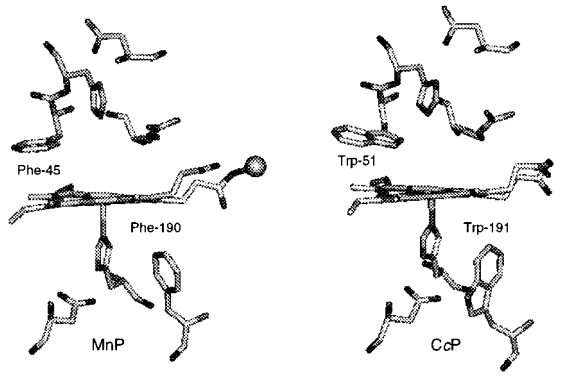

FIGURE 1: Active site structures for MnP and C*c*P.

site in MnP allows it to bind and oxidize Mn(II) to Mn(III). Upon chelation by dicarboxylic acids such as oxalate, the enzymatically generated Mn(III) serves as a diffusable oxidant in the degradation of lignin and small aromatic pollutants. The second manifestation of the structural differences between C*c*P and MnP is the nature of the high-valent intermediates formed in the catalytic cycle. C*c*P forms an intermediate consisting of a ferryl (Fe(IV)═O) and a tryptophan radical (called compound I′). The corresponding intermediate for MnP (like most other peroxidases) contains a ferryl species and a porphyrin π-cation radical (called compound I).

We are interested in investigating the role of the active site tryptophans in peroxidase activity and employed the protein redesign approach in our studies. This approach has been shown to be a powerful method to elucidate key structural differences between two enzymes (*13*). Like *de novo* protein design (*14*), protein redesign is a minimalist approach that complements the biochemical, spectroscopic, and site-directed mutagenesis studies used to investigate structure ↔ function relationships of native enzymes. We are interested in determining if the *necessary* structural features identified from the study of native enzymes are *sufficient* to confer the structure and function of the enzymes. An advantage of the protein redesign approach lies in the fact that protein redesign builds on an existing protein scaffold. This is important since Nature is known to use only a limited number of protein scaffoldings and yet is able to achieve diverse functions by redesigning the active site.

In our studies, we have utilized cytochrome *c* peroxidase as one of our building blocks. A Mn(II)-binding site was constructed in C*c*P at a similar location as in MnP by introduction of three mutations (Gly41Glu, Val45Glu, His181Asp) (*15, 16*), and the engineered Mn(II)-binding site showed structural properties similar to those of the corresponding site in MnP as characterized by UV−vis and paramagnetic NMR studies (*15, 16*). More importantly, the engineered enzyme showed at least a 5-fold increase in MnP activity compared to WTC*c*P, as measured by its ability to oxidize Mn(II) to Mn(III) (*15*). A detailed paramagnetic ^{1}H NMR study revealed that engineering the Mn(II)-binding site weakened the Fe(III)−N(His) bond strength, relative to the template protein WTC*c*P, so that its bond strength is similar to that of the target protein MnP (*16*). The Fe(III)−N(His) bond strength is known to be important for modulation of the reactivity of the high-valent intermediates in the peroxidase catalytic cycle (*17*). The same protein redesign approach has recently been used by Wilcox et al., who engineered a Mn(II)-binding site at the same location in C*c*P (*18*) using different mutations. Despite the differences in design, the Mn(II)-binding affinity and MnP activity are quite similar for the two systems reported. These results complement the studies of the native enzyme (*10−12, 19−22*) and their mutant forms (*23−25*).

In an effort to increase the catalytic activity of our redesigned C*c*P and improve the structural similarity between MnC*c*P and MnP, we have turned our attention to the second major difference between C*c*P and MnP. While the number of tryptophans (7) and tyrosines (14) in C*c*P is unusually high for a protein of its size (34KD), the fact that MnP lacks tyrosine residues and contains only 1 tryptophan is remarkable. The role of protein radicals in enzymatic catalysis has been well-documented (*26*). The catalytic function of the two active site tryptophans (Trp191 and Trp51) present in C*c*P has been elucidated through extensive biochemical and biophysical studies (*4*). Trp191 has been shown to be the primary location for the amino acid radical in C*c*P through a combination of site-directed mutagenesis and ENDOR spectroscopy (*27−33*). For example, when tryptophan-191 was mutated to phenylanine, a transient compound I was observed (*32*). However, in comparison to other peroxidases

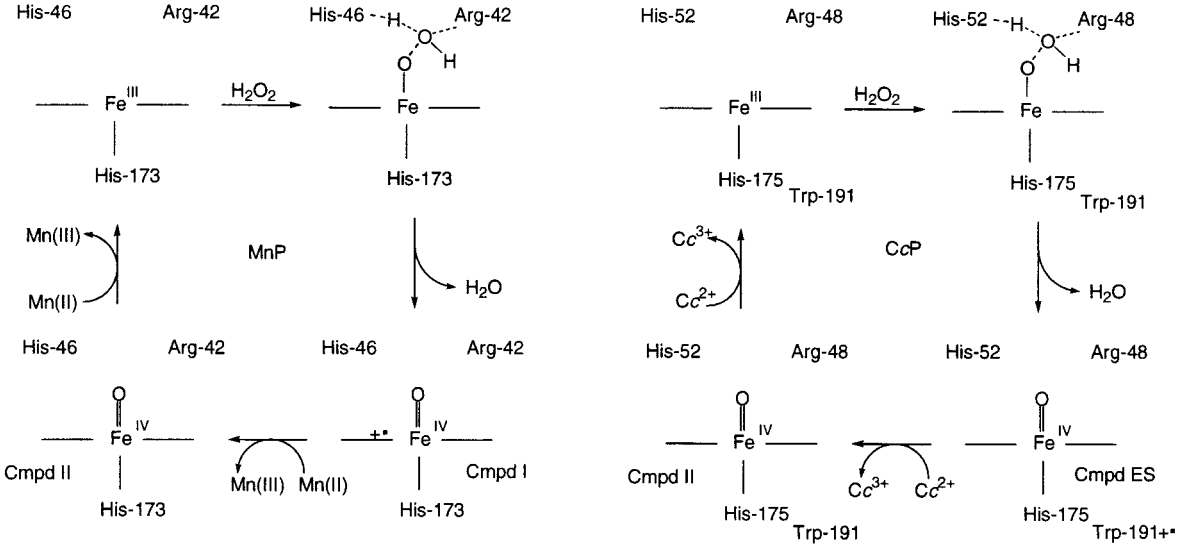

FIGURE 2: The catalytic cycles of MnP and C*c*P.

such as MnP, the C*c*P(MI, W191F) compound I lifetime ($t_{1/2}$ < 14 ms) is extremely short when no substrate is present. Compound I was reduced by an endogenous donor to a ferryl species and unknown amino acid radical (*34*−*37*). While Trp51 is not the primary location of the radical in WTC*c*P containing Trp191, its close proximity to the heme makes it a potential alternate site in C*c*P mutants containing the Trp191Phe mutation. Furthermore, Trp51 has been shown to be important for modulation of the reactivity of compound II (*38*). In this paper, we describe the construction, spectroscopic studies, and functional characterization of MnC*c*P variants containing the Trp191Phe and Trp51Phe mutations. Our results indicate that the two active site tryptophan residues significantly influence the chemistry of the high-valent intermediates and influence MnP activity. More importantly, we have found that the Trp51Phe mutation, and not the Trp191Phe mutation, is responsible for increased MnP activity.

EXPERIMENTAL PROCEDURES

Materials. HPLC purified oligonucleotide primers (50 nmol scale) were ordered from Operon Technologies (Alameda, CA). Native and cloned *Pfu* polymerases were purchased from Stratagene (San Diego, CA). The restriction enzymes *Bgl* II, *Apa* I, *Eco*R I, *Nde* I, and *Kpn* I were purchased from Gibco (Gaithersburg, MD), and *Dpn* I was obtained from Stratagene. T4 DNA ligase was obtained from Gibco. XL-1 Blue and BL-21 cell strains were from Novagen (Madison, WI) and stored as frozen glycerol stocks. DNA purification kits were purchased from Qiagen (Valencia, CA), and the standard protocols contained in the handbooks were followed. A hydrogen peroxide stock solution was stored in the absence of light and the concentration determined by titration against $KMnO_4$ or by UV absorption at 240 nm. Unless otherwise noted, chemicals were obtained from commercial sources and used without further purification.

Protein purification was performed using a Gradi-Frac system from Pharmacia (Piscataway, NJ). DEAE Sepharose CL-6B, Sephacryl H-100, and PD-10 columns were purchased from Pharmacia. Samples were concentrated using YM-10 membranes in a stirred-cell ultrafiltration apparatus or in Centricon-10, both from Amicon (Beverly, MA). Polymerase chain reactions were performed using a PTC-100 thermal cycler from MJ Research (Watertown, MA). Mass spectral analyses were conducted at the University of Illinois Mass Spectroscopy Facility.

Site-Directed Mutagenesis. All site-directed mutagenesis experiments were performed on the C*c*P(MI) gene containing the Met-Ile codon at the N-terminus. The DNA was cloned into a pET-17b plasmid (Novagen, Madison, WI) for site-directed mutagenesis and protein expression. The expressed protein with the Met-Ile at the N-terminus is identical in structural and functional properties to the native yeast C*c*P enzyme (*28*) and is thus called WTC*c*P in this paper. Primers for site-directed mutagenesis were designed with the aid of the Wisconsin GCG Package Version 9.1 (Madison, WI). The plasmid for C*c*P(MI, G41E, V45E, H181D), called MnC*c*P, was constructed as described previously (*15*). The plasmid for C*c*P(MI, W51F, W191F) was constructed from CcP(MI) using two rounds of a PCR mega-primer method (*39*). The Trp191Phe mutation was introduced using an oligonucleotide primer with the sequence 5′-AC GAA GGG CCA TT***C*** GGA GCC G-3′, and the Trp51Phe mutation was introduced using an oligonucleotide primer with the sequence 5′-GA AAT GTG ***GA***A AGC AAG ACG G-3′. Base changes required to change the desired codon are shown in italicized bold type while translationally silent mutations required for restriction digest analysis are shown in bold type. The mutant plasmid for C*c*P(MI, G41E, V45E, H181D, W191F), called MnC*c*P(W191F), was constructed using MnC*c*P plasmid DNA as the template using the PCR mega-primer method. The primer, 5′-AC GAA GGG CCA TT***C*** GGA GCC G-3′ was used to introduce the Trp191Phe mutation. The plasmid for C*c*P(MI, G41E, V45E, W51F, H181D), called MnC*c*P-(W51F), was constructed using the Stratagene QuikChange kit with C*c*P(MI, G41E, V45E, H181D) plasmid DNA serving as the template for the PCR. A set of primers was required to create the mutation with the oligonucleotide 5′-C CGT CTT GCT T***TC*** CAC ATT TCA GG**T** ACC TGG GAC AAG C-3′ and its complement serving as the forward and backward primers, respectively. The silent mutation created a Kpn I restriction site for restriction digest analysis. The plasmid for C*c*P(MI, G41E, V45E, W51F, H181D, W191F), called MnC*c*P(W51F, W191F), was constructed from C*c*P(MI, W51F, W191F) using the Stratagene Quik-Change kit in two steps. The first set of primers, 5′-GCT CTG GGC AAG AC**A** ***G***A***T*** **C**TG AAG AAC TCT GG-3′ and its reverse complement, created the His181Asp mutation. This set of primers contained two translationally silent base changes which were necessary to create a *Bg*l II restriction site and two base changes to change the codon for residue-181. The second primer, 5′-GAC AAC TAT ATA G***AA*** TAT GG**T** CC**G** G***A***A TTA GTC CGT CTT GC-3′ and its reverse complement, created the Gly41Glu and Val45Glu mutations using C*c*P(MI, W51F, H181D, W191F) DNA obtained above as the template. This set of primers removed *Apa* I and *Ban* II restriction sites via translationally silent mutations and changed the desired codon. The standard QuikChange PCR mutagenesis protocol from Stratagen was followed, and the resulting DNA plasmids were screened for the desired mutation by restriction digest analysis. Large quantities of all plasmids were purified from a log-phase culture of *Escherichia coli* XL-1 Blue cells using the Qiagen Midi-Prep kit.

Protein Expression and Purification. Protein expression and purification were carried out as described previously (*15, 16*) with minor modifications. Briefly, the crude lysate was initially purified on a DEAE anion-exchange column using a linear gradient of 14−150 mM KCl in 50 mM KH_2PO_4, pH 7. The apoprotein was further purified on a gel-filtration column with 100 mM KH_2PO_4, pH 7, containing 1 mM EDTA as the elution buffer. Heme was added to the purified apoprotein, and the incorporation process was monitored by UV−visible spectroscopy. After addition of a saturating amount of heme, the mixture was further purified on a DEAE anion exchange column using a linear gradient of 14−150 mM KCl in 50 mM KH_2PO_4, pH 7. Trace metal ion contaminants were removed by dialysis against two changes of 50 mM KH_2PO_4, pH 7, containing 10 mM EDTA, two changes of 50 mM KH_2PO_4, pH 7, 100 mM KCl, and two changes of 50 mM KH_2PO_4, pH 7. The homogeneity of the protein was confirmed by denaturing gel electrophoresis, and the molecular weight was determined by electrospray mass

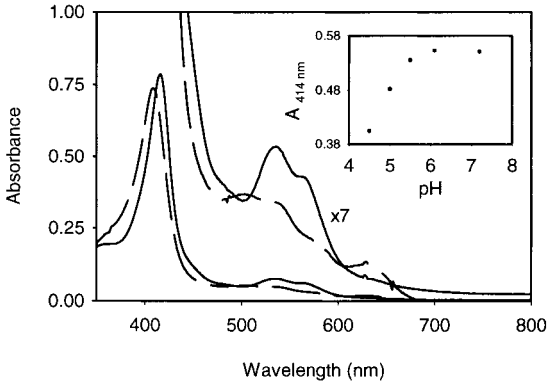

FIGURE 3: UV−vis spectra for MnC*c*P(W191F) at pH 5 (dashed line) and pH 7 (solid line).

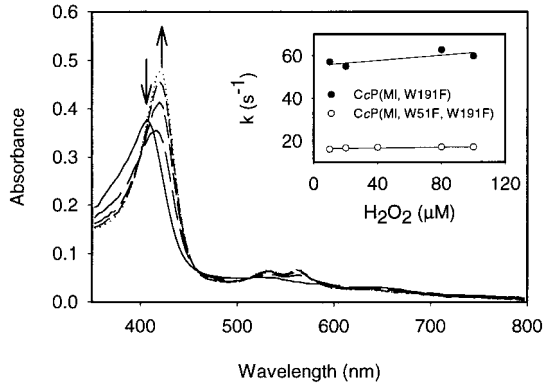

FIGURE 4: Stopped-flow UV−vis spectra for formation and decay of compound I in C*c*P(MI, W191F). Spectra shown are for 3.8 (solid line), 14.1 (long dashed), 24.3 (medium dashed), 34.6 (short dashed), and 44.8 ms (dotted) after initiation of the reaction. Inset: Rate of compound I decay for C*c*P(MI,W191F) and C*c*P(MI, W51F, W191F) as a function of hydrogen peroxide concentration. The samples were in 100 mM KH_2PO_4, pH 6 (ionic strength), and reactions were performed at 25 °C.

spectrometry. The observed molecular weights for the mutant proteins match the calculated molecular weights within experimental error. Molar extinction coefficients were estimated using the pyridine hemochromagen method (*40*, *41*).

Mn(II) Oxidation. Mn(II) oxidation assays were performed using a HP 8453 diode-array spectrophotometer equipped with a PolyScience water bath. All kinetic assays were performed at 25 °C. The oxidation of Mn(II) was monitored following the increase in absorption at 270 nm due to the formation of Mn(III) malonate (*19*, *20*, *42*). An extinction coefficient of 11.9 mM^{-1} cm^{-1} was used in the calculations. For determination of the apparent Michaelis−Menton parameters for Mn(II), typical assay solutions contained 0.6 μM enzyme and 0.8−27 mM Mn(II) in 500 mM malonate buffer at pH 5 and the reactions were initiated by addition of hydrogen peroxide to a final concentration of 0.1 mM. Lineweaver−Burk plots (Figure 5) were constructed using the linear portion of the kinetic traces (Supporting Information). The data presented are the average of at least three measurements, and error bars are shown in the corresponding figures.

Stopped-Flow Kinetics. Stopped-flow UV−vis spectra were collected using an Applied Photophysics Ltd (Leatherhead, U.K.) SX18.MV stopped-flow spectrometer equipped with a 256 element photodiode array detector and a two-syringe sequential mixer encased in a thermostated water

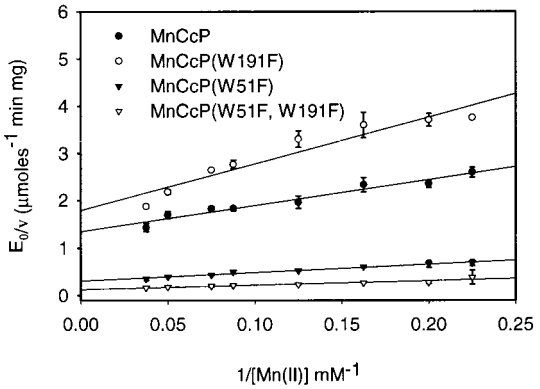

FIGURE 5: Lineweaver−Burk plots for Mn(II) oxidation by MnC*c*P, MnC*c*P(W191F), MnCcP(W51F), and MnC*c*P(W51F, W191F). Assay conditions were as described in the text.

bath. Reactions were carried out at 25 °C. Enzyme samples were prepared in 500 mM malonate, pH 5. Hydrogen peroxide samples in 500 mM malonate were prepared from a concentrated stock solution. Spectra were collected on a logarithmic basis for the first 10 s after mixing. Spectra were analyzed using the program Pro-Kineticist (Applied Photophysics Ltd.).

RESULTS

pH-Dependent UV−Vis Spectra. The UV−vis spectra for MnC*c*P(W51F, W191F) at pH 5 and 7 are shown in Figure 3. At pH 7, the protein displayed a Soret band at 414 nm and α and β bands at 565 and 536 nm, typical of low-spin ferric heme. At pH 5, the Soret band blue-shifted to 408 nm and new bands at 500 and 574 nm and a charge-transfer band at 635 nm appeared, indicating that mainly a high-spin heme species exists in solution at this pH. The insert of Figure 3 displays the pH-dependent spin state transition as monitored by absorption at 414 nm. The spectra and the pH-dependent changes observed for MnC*c*P(W191F) were almost identical to those observed for MnC*c*P(W51F, W191F) (data not shown). This pH-dependent spin state change does not occur for WTC*c*P (*43*) but has been observed for most C*c*P mutants including all mutants containing the engineered Mn(II)-binding site (*15*, *16*, *18*).

Kinetics of Compound I Formation and Decay. By introduction of Trp191Phe mutation into C*c*P(MI), Erman et al. detected transient formation of compound I using stopped-flow UV−vis spectroscopy (*32*). However, compound I rapidly decayed to ferryl and another protein radical with a rate of 51 s^{-1} (*32*). In this study, we further introduced a Trp51Phe mutation and compared the effect of both a Trp191Phe single mutation and a Trp191Phe/Trp51Phe double mutation on compound I decay. The spectral change upon addition of H_2O_2 to C*c*P(MI, W191F) (shown in Figure 4) and to C*c*P(MI, W51F, W191F) (data not shown) are similar to that obtained by Erman et al. (*32*). As shown in the insert of Figure 4, the rate of compound I decay of both the single and the double mutants are expectedly independent of H_2O_2 concentration. More importantly, the results demonstrated that the Trp191Phe and Trp51Phe mutations resulted in a more stable compound I, with a compound I decay rate of 18 s^{-1} for C*c*P(MI, W51F, W191F) compared to 60 s^{-1} for C*c*P(MI, W191F).

Table 1: Apparent Steady-State Kinetic Parameters for MnC*c*P, MnC*c*P(W191F), MnC*c*P(W51F), and MnC*c*P(W51F, W191F)[a]

enzyme	V_{max} (μmol min^{-1} mg^{-1})	K_M (mM)	k_{cat} (s^{-1})	k_{cat}/K_M (s^{-1} mM^{-1})
MnC*c*P	0.75	4.1	0.42	0.102
MnC*c*P(W191F)	0.56	5.6	0.32	0.057
MnC*c*P(W51F)	3.20	5.6	1.83	0.327
MnC*c*P(W51F, W191F)	8.00	7.6	4.55	0.599
MnP	377.4	0.0732	289.3	3952

[a] Assays for MnCcP mutants were performed in 500 mM malonate buffer at pH 5. MnP parameters are taken from ref *18* and were obtained in 50 mM malonate at pH 4.5. The activity difference between the MnC*c*P mutants and MnP shown in the table is smaller if compared at the same pH (see text for details).

Steady-State Kinetics. Mn(II) oxidation assays on MnC*c*P(W191F), MnC*c*P(W51F), and MnC*c*P(W51F, W191F) were performed at pH 5 in 500 mM malonate buffer. Under conditions of saturating hydrogen peroxide, the MnC*c*P mutants displayed saturation behavior with respect to Mn(II). The Lineweaver−Burk plots for the three new mutants and MnC*c*P under conditions of saturating hydrogen peroxide are shown in Figure 5. The kinetic parameters extracted from these plots are compiled in Table 1. The MnP specific activity, defined as the number of micromoles of Mn(II) oxidized per milligram protein per minute, was 0.750 μmol min^{-1} mg^{-1} for MnC*c*P at pH 5. A slight decrease in activity was observed for MnC*c*P(W191F) (0.591 μmol min^{-1} mg^{-1}) while MnC*c*P(W51F) and MnC*c*P(W51F, W191F) displayed significantly increased specific activity (3.20 and 8.00 μmol min^{-1} mg^{-1}, respectively). The apparent k_{cat} values followed a trend similar to that observed for specific activity, while the apparent K_m values varied slightly from 4.1 mM for MnC*c*P to 7.6 mM for MnC*c*P(W51F, W191F). Therefore, a 2-fold decrease (compared to MnC*c*P) in k_{cat}/K_m was observed for MnC*c*P(W191F), while MnC*c*P(W51F) and MnC*c*P(W51F, W191F) exhibited 3- and 6-fold increases in k_{cat}/K_m, respectively. Interestingly, the introduction of the Trp51Phe mutation caused a greater relative increase in activity when the Trp191Phe mutation was already present. The increase in the apparent k_{cat} for MnC*c*P(W51F) compared to MnC*c*P was 4-fold while the increase for MnC*c*P(W51F, W191F) compared to MnC*c*P(W191F) was 14-fold.

Steady-State UV−Vis Spectral Characterization. To offer mechanistic insight into the role of Trp191 and Trp51 in the MnP activity, steady-state UV−vis spectra were collected during the oxidation of Mn(II) by our MnC*c*P mutants (Figure 6). The UV−vis spectrum of resting state MnC*c*P in the presence of excess Mn(II) contained a Soret maximum at 408 nm and a CT band at 630 nm. After addition of hydrogen peroxide to initiate catalytic turnover, the Soret band red-shifted to 416 nm and decreased in intensity slightly. The α, β bands (560 and 530 nm, respectively) became sharper, and the CT band decreased in intensity. The spectra observed for MnC*c*P(W191F), MnC*c*P(W51F), and MnC*c*P(W51F, W191F) under steady-state conditions were qualitatively similar (data not shown).

Under the experimental conditions employed here, compound II and/or compound III could form. Compound II is known to be an active species in the catalytic cycle of peroxidases. The catalytically inactive species, compound III, forms by the reaction of compound II with excess peroxide. The spectral features we observed are consistent with the formation of compound II (*32*) since compound III is characterized by α and β bands at 578 and 545 nm while α and β bands at 560 and 530 nm are typical of a compound II (*10*). Furthermore, when Mn(II) oxidation assays were performed using a subsaturating concentration of hydrogen peroxide, the steady-state intermediate spectrum was observed to decay back to a resting state spectrum during the assay (data not shown). At the time the decay of the intermediate was observed, product formation, as monitored by the absorption at 270 nm due to Mn(III) malonate, was observed to cease. Product formation could be reinitiated by the addition of hydrogen peroxide and the steady-state spectrum returned. Since catalysis correlated with the presence of the intermediate described above, the intermediate observed is catalytically active. These observations suggest that the active intermediate compound II, and not compound III, accumulated during turnover for all four MnCcP mutants.

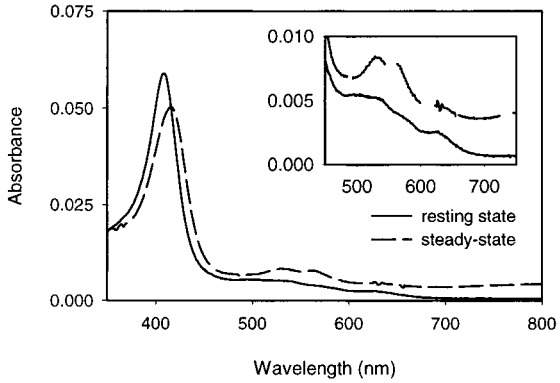

FIGURE 6: UV−visible spectra for MnC*c*P in 500 mM malonate pH 5 in the presence of Mn(II) before and after addition of hydrogen peroxide to initiate steady-state catalysis.

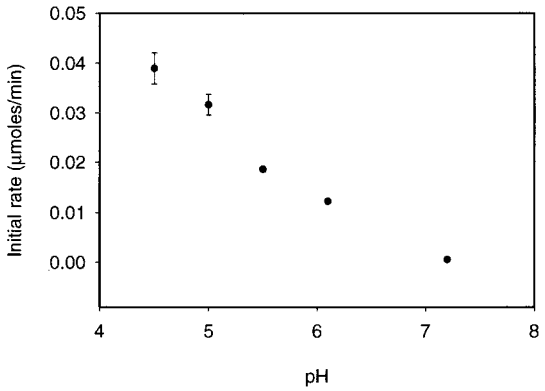

FIGURE 7: Initial rate of Mn(II) oxidation by MnC*c*P(W51F, W191F) as a function of pH. Reactions consisted of 140 μM enzyme and 13.3 mM Mn(II) and were initiated by addition of hydrogen peroxide to a concentration of 0.1 mM.

pH Dependence of MnP Activity. MnP is known to have a low pH optimum, achieving the highest activity at pH 4.5 (*44*). To investigate whether the engineered C*c*P mutants also have similar low pH optima, Mn(II) oxidation was performed for MnC*c*P(W51F, W191F) at pH 4.5, 5, 5.5, 6.1, and 7.2. As shown in Figure 7, the initial rate of Mn(II) oxidation increases with decreasing pH, similar to that observed in MnP.

DISCUSSION

Structural comparisons reveal two major differences between C*c*P and MnP that should contribute to the

functional differences (Figure 1). While MnP contains a Mn(II)-binding site, C*c*P does not bind Mn(II). The critical role of the Mn(II)-binding site in MnP activity was first elucidated by biochemical studies (*10*−*12*, *19*−*22*), confirmed by site-directed mutagenesis (*23*−*25*), and firmly established when a Mn(II)-binding site was engineered into C*c*P by our lab (*15*, *16*) and by Wilcox et al. (*18*). As shown in Figure 1, one of the heme propionates is a ligand for Mn(II) and therefore provides a direct pathway for the oxidation of Mn(II). Engineering a Mn(II)-binding site in C*c*P restores this pathway for Mn(II) oxidation in C*c*P and thus is responsible for the increased MnP activity of MnC*c*P.

The role of the disparaging number of redox active amino acids, such as the active site tryptophans, is not as clear. As shown in Figure 2, both enzymes react with H_2O_2 to form high-valent intermediates. The first intermediate detected for WTC*c*P, compound I′, contains a ferryl oxo, tryptophan radical and oxidizes 1 equiv of ferrocytochrome *c* to give ferricytochrome *c* and compound II. The catalytic cycle is completed by oxidation of a second 1 equiv of ferrocytochrome *c* by compound II. On the other hand, MnP forms the more common intermediate, compound I, which consists of a ferryl oxo and porphyrin π cation radical and oxidizes Mn(II) to Mn(III). Like C*c*P, the catalytic cycle is completed by oxidation of a second 1 equiv of Mn(II) by compound II.

While the redox active amino acids Trp191 and Trp51 have been shown to play a critical role in long-range electron transfer between cytochrome *c* and C*c*P (*4*, *36*, *45*), they are not present in MnP and may be deleterious to MnP activity. Since MnC*c*P contains Trp191, the enzyme will form compound I′ in the catalytic cycle, which may not be as efficient an oxidant of Mn(II) as compound I. Trp51 and Trp191 may facilitate "leakage" of oxidizing equivalents from compound I′ and compound II to other protein residues and thereby decrease the catalytic efficiency of manganese oxidation by MnC*c*P.

Oxidation of WTC*c*P residues during its reaction with hydrogen peroxide has been reported. Erman observed C*c*P dimerization through oxidized tyrosine residues (*34*), and English reported the loss of tryptophan and tyrosine residues as a result of the treatment of C*c*P with excess hydrogen peroxide (*35*, *37*). By replacing Phe with Trp in horseradish peroxidase at the corresponding position of Trp191 in C*c*P, Morimoto et al. observed spectral features corresponding a ferryl and a Trp radical (*46*). This oxidative "leakage" could decrease catalytic efficiency if it were to occur during catalysis. The absence of tyrosines and tryptophans in MnP should limit the extent of such side reactions.

Interestingly, ascorbate peroxidase (APX) also contains a proximal Trp residue at the corresponding position of Trp191 in C*c*P (*47*), and yet APX forms compound I intermediate instead of compound I′ found in C*c*P (*48*). The difference between APX and C*c*P has been attributed to the presence of a cation-binding site that is ~8 Å away from the proximal Trp in APX (*49*, *50*). This cation-binding site is believed to raise the reduction potential of the proximal Trp through electrostatic interaction and therefore preventing the generation of compound I′. The cation-binding site is absent in C*c*P. Introduction of the cation-binding site in C*c*P resulted in destabilization of compound I′ (*51*). However, for the majority of peroxidases such as horseradish peroxidase and MnP, the strategy to prevent compound I′ formation is the replacement of the proximal Trp residue with a Phe, which is more difficult to oxidize. Therefore, we have incorporated the Trp191Phe single mutation and Trp191Phe/Trp51Phe double mutations into WTC*c*P to investigate their roles in compound I formation and decay. The same mutations were engineered into MnC*c*P to examine their effect on the MnP activity of our MnC*c*P mutants. As first observed by Erman et al. (*32*) and reproduced by us, stopped-flow UV−visible data for the reaction of C*c*P(MI, W191F) with hydrogen peroxide suggest that the W191F mutation results in transient formation of compound I. Furthermore, our results show that the double mutant C*c*P(MI, W51F, W191F) exhibits a longer lived compound I (decay rates: C*c*P(MI, W191F), 60 s^{-1}; C*c*P(MI, W51F, W191F), 18 s^{-1}). For C*c*P(MI, W191F) and C*c*P(MI, W51F, W191F), the transiently formed compound I decays to a species containing a ferryl oxo and protein radical. The location(s) of this radical in C*c*P mutants containing the Trp191Phe mutation has not been unambiguously identified (*34*−*37*, *52*). Although Trp51 has been ruled out as the *primary* radical site in WTC*c*P, its close position to the heme makes it an attractive site for the radical in the W191F mutants. Our observation that compound I decays slower in C*c*P(MI, W51F, W191F) suggests that Trp-51 may be an alternate radical site for C*c*P mutants lacking Trp-191.

Addition of the Trp191Phe mutation to MnC*c*P should lead to a significant increase in activity if formation of compound I is responsible for the ability of MnP to oxidize Mn(II). However, a small decrease in Mn(II) oxidation activity was observed for MnC*c*P(W191F) relative to MnC*c*P despite the fact that MnC*c*P(W191F) forms compound I instead of compound I′. In addition, the buildup of compound II under steady-state conditions for both enzymes requires that the Trp191Phe mutation does not change the rate-limiting step in manganese oxidation. Our results suggest that the nature of the first high-valent intermediate is not critical to manganese oxidation. While the Trp191Phe mutation expectedly allows for detection of compound I by preventing leakage of the porphyrin π-cation radical to tryptophan-191 and thereby increasing compound I lifetime, the length of compound I lifetime (in the absence of reducing substrate) appears to have little effect on MnP activity.

As shown in Figure 2, catalytic turnover by peroxidases requires the reaction of compound II with substrate for both C*c*P and MnP. It has been shown that the reaction of compound II with its respective substrate (cytochrome *c* for C*c*P and Mn(II) for MnP) is the rate-limiting step for both C*c*P (*4*, *53*) and MnP (*10*, *11*, *19*, *20*). Therefore, even though compound I most likely reacts significantly faster than compound I′, the reaction of compound II with manganese should determine the overall reaction rate. Our observation of compound II during the steady-state assays indicates that any improvements in catalytic activity must be due to modulation of the reactivity of compound II. The observation of similar activity for MnC*c*P and MnC*c*P(W191F), but significantly improved activity for MnC*c*P(W51F) and MnC*c*P(W51F, W191F), supports the conclusion that Trp191 has little influence on compound II reactivity. Therefore, in addition to influencing the lifetime of compound I, the Trp51Phe mutation most likely affects the reactivity of compound II. The role of tryptophan-51 had been investigated previously. C*c*P mutants containing either the Trp51Ala

or Trp51Phe mutations were shown to exhibit increased activity toward small aromatic substrates (*38*). It was proposed that Trp51 stabilizes C*c*P compound II via a hydrogen bonding interaction with the ferryl oxygen. These results, and our results with the MnC*c*P mutants, suggest the Trp51Phe mutation increases the MnP activity by increasing the rate of reaction of compound II with manganese.

Interestingly, like in MnP, the catalytic activity of MnC*c*P(W191F) and MnC*c*P(W51F, W191F) increases with decreasing pH (see Figure 7). This trend may reflect the increasing redox potentials of reaction intermediates with decreasing pH observed for numerous peroxidases (*54*, *55*). However, the search for the origin of pH-dependent activity shown in Figure 7 is complicated by the pH-dependent spin state change in MnCcP that is absent in MnP. As shown in Figure 3, the MnC*c*P mutants at high pH are low-spin as a result of coordination of either distal histidine or hydroxide as a sixth ligand (*16*). At lower pH, a high-spin species predominates, consistent with either loss of a coordinated histidine or protonation of the coordinated hydroxide resulting in a more labile aquo ligand. Regardless of the nature of the sixth ligand in the low-spin form, the low spin form reacts slowly with hydrogen peroxide. Therefore, the pH-dependent activity shown in Figure 7 is a combination of both pH-dependent reactivity of enzyme intermediates and pH-dependent spin state change. Since the approximately linear trend shown in Figure 7 does not match the sigmoidal curve shown in the insert of Figure 3, it is expected that the pH-dependent spin state change is not a dominant factor in the pH-dependent activity shown in Figure 7.

While the improvement in activity observed for MnC*c*P(W51F, W191F) compared to WTC*c*P is significant, comparison of the kinetic parameters for Mn(II) oxidation for MnP and MnC*c*P(W51F, W191F) shows our mutant to be ~47-fold less in specific activity and ~6600 times less efficient in k_{cat}/K_M. This is a result of the combination of an ~64-fold less k_{cat} and an ~100-fold larger K_M. In should be noted that MnP activity was determined at pH 4.5, while the activity of the MnC*c*P mutants reported herein was determined at pH 5. We chose pH 5 to characterize our MnC*c*P mutants because at this pH the initial linear portion of kinetic trace persists for a longer period of time and thus the results are more reliable. Since MnC*c*P(W51F, W191F) appears more active at a lower pH than used in our assays (see Figure 7), the quantitative differences noted above should be taken as an upper limit.

In summary, we have introduced Trp191Phe and Trp51Phe mutations to our engineered Mn(II)-binding enzyme, MnC*c*P, in an effort to increase the MnP activity of our engineered MnP model. While the Trp191Phe mutation increases the lifetime of compound I, it does not influence the reactivity of compound II. Utilization of compound I′ instead of compound I for manganese oxidation does not influence the overall catalytic efficiency or change the rate-limiting step in the catalytic cycle. Further introduction of the Trp51Phe mutation not only increases the lifetime of compound I in the absence of substrate but also increases the reactivity of compound II and thus MnP activity. MnC*c*P(W51F, W191F) exhibits the highest Mn(II) oxidation activity for a C*c*P mutant constructed and characterized to date.

Three strategies exist to further improve the catalytic efficiency exhibited by C*c*P mutants capable of oxidizing Mn(II). First, the design of the metal-binding site could be reexamined and improved. The second approach would focus on trying to improve the turnover rate of the engineered enzymes by influencing the reactivity of the two high-valent intermediates. Specifically, since the reaction of compound II with manganese is rate limiting in the catalytic cycle, efforts should be focused on modulating the properties and reactivity of this intermediate. Redox active amino acids (Trp and Tyr) at other locations may also play important roles in influencing MnP activity. Finally, modulation of the pK_a for the pH-dependent spin state transition may lead to enzymes with higher activity at higher pH. Progress is being made toward addressing these issues.

ACKNOWLEDGMENT

We thank Bryan K. S. Yeung for initial work on this project, Professor Robert B. Gennis for use of the stopped-flow spectrophotometer, and Professors Robert B. Gennis and Lowell P. Hager for helpful discussions.

SUPPORTING INFORMATION AVAILABLE

One figure displaying typical kinetic traces for the oxidation of Mn(II) by MnC*c*P, MnC*c*P(W191F), MnC*c*P(W51F), and MnC*c*P(W51F, W191F). This material is available free of charge via the Internet at http://pubs.acs.org.

REFERENCES

1. Everse, J., Everse, K. E., and Grisham, M. B. (1990) *Peroxidases in Chemistry and Biology*, CRC Press, Boca Raton, FL.
2. Welinder, K. G. (1992) *Curr. Opin. Struct. Biol. 2*, 388−393.
3. Poulos, T. L., and Fenna, R. E. (1994) *Met. Ions Biol. Syst. 30*, 25−75.
4. English, A. M., and Tsaprailis, G. (1995) *Adv. Inorg. Chem. 43*, 79−125.
5. Poulos, T. L., and Kraut, J. (1980) *J. Biol. Chem. 255*, 8199−8205.
6. Finzel, B. C., Poulos, T. L., and Kraut, J. (1984) *J. Biol. Chem. 259*, 13027−13036.
7. Edwards, S. L., and Poulos, T. L. (1990) *J. Biol. Chem. 265*, 2588−2595.
8. Sundaramoorthy, M., Kishi, K., Gold, M. H., and Poulos, T. L. (1994) *J. Biol. Chem. 269*, 32759−32767.
9. Bosshard, H. R., Anni, H., and Yonetani, T. (1991) in *Peroxidases in Chemistry and Biology* (Everse, J., and Grisham, M. B., Eds.) pp 51−84, CRC Press, Boca Raton, FL.
10. Gold, M. H., Wariishi, H., and Valli, K. (1989) *ACS Symp. Ser. 389*, 127−140.
11. Cai, D., and Tien, M. (1993) *J. Biotechnol. 30*, 79−90.
12. Stahl, J. D., and Aust, S. D. (1998) *Rev. Toxicol. (Amsterdam) 2*, 189−194.
13. Lu, Y., and Valentine, J. S. (1997) *Curr. Opin. Struct. Biol. 7*, 495−500.
14. Bryson, J. W., Betz, S. F., Lu, H. S., Suich, D. J., Zhou, H. X., Oneil, K. T., and Degrado, W. F. (1995) *Science 270*, 935−941.
15. Yeung, B. K., Wang, X., Sigman, J. A., Petillo, P. A., and Lu, Y. (1997) *Chem. Biol. 4*, 215−221.
16. Wang, X., and Lu, Y. (1999) *Biochemistry 38*, 9146−9157.
17. Banci, L., Bertini, I., Turano, P., Tein, M., and Kirk, T. K. (1991) *Proc. Natl. Acad. Sci. U.S.A. 88*, 6956−6960.
18. Wilcox, S. K., Putnam, C. D., Sastry, M., Blankenship, J., Chazin, W. J., McRee, D. E., and Goodin, D. B. (1998) *Biochemistry 37*, 16853−16862.

19. Wariishi, H., Valli, K., and Gold, M. H. (1992) *J. Biol. Chem. 267*, 23688−23695.
20. Kuan, I. C., Johnson, K. A., and Tien, M. (1993) *J. Biol. Chem. 268*, 20064−20070.
21. Timofeevski, S. L., and Aust, S. D. (1997) *Biochem. Biophys. Res. Commun. 239*, 645−649.
22. Mauk, M. R., Kishi, K., Gold, M. H., and Mauk, A. G. (1998) *Biochemistry 37*, 6767−6771.
23. Kishi, K., Kusters-van Someren, M., Mayfield, M. B., Sun, J., Loehr, T. M., and Gold, M. H. (1996) *Biochemistry 35*, 8986−8994.
24. Whitwam, R. E., Brown, K. R., Musick, M., Natan, M. J., and Tien, M. (1997) *Biochemistry 36*, 9766−9773.
25. Sundaramoorthy, M., Kishi, K., Gold, M. H., and Poulos, T. L. (1997) *J. Biol. Chem. 272*, 17574−17580.
26. Stubbe, J., and van der Donk, W. A. (1998) *Chem. Rev. 98*, 705−762.
27. Edwards, S. L., Xuong, N., Hamlin, R. C., and Kraut, J. (1987) *Biochemistry 26*, 1503−1511.
28. Fishel, L. A., Villafranca, J. E., Mauro, J. M., and Kraut, J. (1987) *Biochemistry 26*, 351−360.
29. Fishel, L. A., Farnum, M. F., Mauro, J. M., Miller, M. A., Kraut, J., Liu, Y., Tan, X., and Scholes, C. P. (1991) *Biochemistry 30*, 1986−1996.
30. Goodin, D. B., Mauk, A. G., and Smith, M. (1987) *J. Biol. Chem. 262*, 7719−7724.
31. Mauro, J. M., Fishel, L. A., Hazzard, J. T., Meyer, T. E., Tollin, G., Cusanovich, M. A., and Kraut, J. (1988) *Biochemistry 27*, 6243−6256.
32. Erman, J. E., Vitello, L. B., Mauro, J. M., and Kraut, J. (1989) *Biochemistry 28*, 7992−7995.
33. Sivaraja, M., Goodin, D. B., Smith, M., and Hoffman, B. M. (1989) *Science (Washington, D.C.) 245*, 738−740.
34. Spangler, B. D., and Erman, J. E. (1986) *Biochim. Biophys. Acta 872*, 155−157.
35. Fox, T., Tsaprailis, G., and English, A. M. (1994) *Biochemistry 33*, 186−191.
36. Miller, M. A., Vitello, L., and Erman, J. E. (1995) *Biochemistry 34*, 12048−12058.
37. Tsaprailis, G., and English, A. M. (1996) *Can. J. Chem. 74*, 2250−2257.
38. Roe, J. A., and Goodin, D. B. (1993) *J. Biol. Chem. 268*, 20037−20045.
39. Sarkar, G., and Sommer, S. S. (1990) *BioTechniques 8*, 404−407.
40. De Duve, C. (1948) *Acta Chem. Scand. 2*, 264−289.
41. Morrison, M., and Horie, S. (1965) *Anal. Biochem. 12*, 77−82.
42. Khindaria, A., Barr, D. P., and Aust, S. D. (1995) *Biochemistry 34*, 7773−7779.
43. Vitello, L. B., Huang, M., and Erman, J. E. (1990) *Biochemistry 29*, 4283−4288.
44. Glenn, J. K., and Gold, M. H. (1985) *Arch. Biochem. Biophy. 242*, 329−341.
45. Pelletier, H., and Kraut, J. (1992) *Science 258*, 1748−1755.
46. Morimoto, A., Tanaka, M., Takahashi, S., Ishimori, K., Hori, H., and Morishima, I. (1998) *J. Biol. Chem. 273*, 14753−14760.
47. Patterson, W. R., and Poulos, T. L. (1995) *Biochemistry 34*, 4331−4341.
48. Patterson, W. R., Poulos, T. L., and Goodin, D. B. (1995) *Biochemistry 34*, 4342−4345.
49. Poulos, T. L., Patterson, W. R., and Sundaramoorthy, M. (1995) *Biochem. Soc. Trans. 23*, 228−232.
50. Nissum, M., Neri, F., Mandelman, D., Poulos, T. L., and Smulevich, G. (1998) *Biochemistry 37*, 8080−8087.
51. Bonagura, C. A., Sundaramoorthy, M., Pappa, H. S., Patterson, W. R., and Poulos, T. L. (1996) *Biochemistry 35*, 6107−6115.
52. Musah, R. A., and Goodin, D. B. (1997) *Biochemistry 36*, 11665−11674.
53. Matthis, A. L., Vitello, L. B., and Erman, J. E. (1995) *Biochemistry 34*, 9991−9999.
54. Purcell, W. L., and Erman, J. E. (1976) *J. Am. Chem. Soc. 98*, 7033−7037.
55. Hayashi, Y., and Yamazaki, I. (1979) *J. Biol. Chem. 254*, 9101−9106.

BI990666+